第 35 卷第 10 期 无 机 化 学 学 报 Vol.35 No.10
2019 年 10 月 CHINESE JOURNAL OF INORGANIC CHEMISTRY 1885-1895

不同氧化硅前驱体熔盐反应制备莫来石晶须

马雪冬[1,2] 韩霁昌[2] 杜 炜[1] 王 伟*[,1,3]
([1]长安大学环境科学与工程学院,旱区地下水文与生态效应教育部重点实验室,西安 710054)
([2]国土资源部退化及未利用土地整治工程重点实验室,西安 710075)
([3]长安大学,陕西省土地整治重点实验室,西安 710054)

摘要:利用熔盐反应制备了莫来石晶须,采用 X 射线粉末衍射(XRD)、扫描电子显微镜(SEM)、热重分析(TG-DSC)、高分辨透射电镜(HRTEM)等分析表征技术对所制备的莫来石晶须进行了测定。SEM 研究表明莫来石晶须的直径在 200~400 nm 范围,长度可达到几个微米。HRTEM 照片显示所制备晶须的晶面间距为 0.539 nm,正好与莫来石(110)晶面数据吻合,证明熔盐法制备的晶须为莫来石。随着反应物中氧化硅物种的引入,γ-Al_2O_3 不断消耗和莫来石相不断生长,获得了各向异性的莫来石晶须。硫酸铝的分解反应是最重要的反应控制步骤,如果没有硅物种参与反应,可以在 900 ℃下硫酸钠–硫酸铝的复合熔盐体系中得到 α-Al_2O_3。熔盐反应的热力学计算表明,相比于 γ-Al_2O_3,α-Al_2O_3 作为硫酸铝分解的产物具有更稳定的能态。采用 Kissinger-Akahira-Suno 方法对硫酸铝分解过程的动力学进行研究,硫酸铝分解反应的表观活化能(E_a)为 257.2 kJ·mol^{-1}。

关键词:熔盐合成;莫来石晶须;热分解;表观活化能
中图分类号:O611.4;TB34 文献标识码:A 文章编号:1001-4861(2019)10-1885-11
DOI:10.11862/CJIC.2019.216

Preparation and Characterization of Mullite Whiskers from Different Silica Sources via Molten Salt Reaction

MA Xue-Dong[1,2] HAN Ji-Chang[2] DU Wei[1] WANG Wei*[,1,3]
([1]*College of Environment Science and Engineering, Key Laboratory of Subsurface Hydrology and Ecology in Arid Areas, Ministry of Education, Chang'an University, Xi'an* 710054, *China*)
([2]*Key Laboratory of Degraded and Unused Land Consolidation Engineering, the Ministry of Land and Resources of China, Xi'an* 710075, *China*)
([3]*Shaanxi Key Laboratory of Land Consolidation, Chang'an University, Xi'an* 710054, *China*)

Abstract: Mullite whiskers were prepared using molten salt reaction. The resulting whiskers have been investigated by X-ray diffraction (XRD), scanning electron microscopy (SEM), thermogravimetric analysis (TG-DSC) and high resolution transmission electron microscopy (HRTEM). SEM studies showed that diameter of the mullite whiskers was in a range of 200~400 nm and their length was several microns. The analysis of HRTEM data revealed that the interplanar spacing was 0.539 nm, in accordance with the spacing of (110) crystal plane of mullite. As silica species was introduced into starting reactants, the combination reaction of mullite formation took place, γ-Al_2O_3 was consumed and mullite whiskers grew continuously. The most important factor in controlling mullite formation is the decomposition reaction of aluminum sulfate, and α-Al_2O_3 is fabricated by thermal pyrolysis of aluminum sulfate at 900 ℃ in molten sodium sulfate system without silica species

收稿日期:2019-05-13。收修改稿日期:2019-08-11。
国家自然科学基金(No.51678059),陕西省重点研发计划(No.2019GY-179),国土资源部退化及未利用土地整治工程重点实验室开放基金(No.SXDJ2017-1),陕西省土地整治重点实验室开放基金项目(No.2018-JC10)和中央高校基本科研业务费(No.300102298202)资助。
*通信联系人。E-mail:wwchem@chd.edu.cn

participating. According to the thermodynamic calculation, α-Al_2O_3 is a stable phase as the product of the decomposition of $Al_2(SO_4)_3$ in comparison to γ-Al_2O_3, and mullite formation reaction is a spontaneous process in the whole temperature range. The decomposition reaction of aluminum sulfate was investigated by Kissinger-Akahira-Suno method with various heating rates (β=5, 10 and 15 K·min^{-1}), and the apparent activation energy (E_a) of reaction is 257.2 kJ·mol^{-1}.

Keywords: molten salt synthesis; mullite whiskers; thermal pyrolysis; apparent activation energy

0 Introduction

Mullite is a strong candidate material for advanced structural applications at high temperature, because of its low thermal expansion, low thermal conductivity, high temperature creep resistance, good chemical and thermal stability[1]. Mullite is the only stable compound in the Al_2O_3-SiO_2 system at atmosphere pressure, and it is a peritectic phase, but under certain conditions it can solidify metastable without prior alumina nucleation. The crystal structure of mullite is orthorhombic and is generally viewed as a defect from sillimanite, $Al_2O_3 \cdot SiO_2$. The mullite structure consists of chains of edge-sharing AlO_6 octahedra running parallel to the *c*-axis. These chains are cross-linked by alternating (Si, Al)O_4 tetrahedra forming chains, which also run parallel to the *c*-axis[2]. Each octahedron shares two oxygen atoms, along an edge, with the octahedron just above it. And the tetrahedra share corner atoms in both the *ab*-plane (forming the double-chain) and the *c*-axis. Because the tetrahedrally coordinated aluminium and silicon are no longer present in the ratio of 1:1, these sites necessarily become chemically disordered. Furthermore, crystal structure analysis have identified the presence of a second tetrahedral site-displaced from the original by approximately 0.13 nm, whch is presumably occupied by cations that have lost bridging O atoms[3]. Ghate et al. firstly reported kinetics of mullite about densification and grain growth[4]. They assumed that diffusion of Si^{4+} controlled densification and grain growth process. Some research literatures reveal that the needle-like shape is common to mullite formed in the presence of a liquid, whereas sintering of Al_2O_3-SiO_2 compounds in the absence of liquid cerated aggregates or agglomerations of mullite. In the case of acicular grain growth, mullite whiskers grow in the *c*-axis direction and are bounded by (110) surfaces. It is believed that the prismatic (110) planes have a lower surface energy than *c*-axis growth, and thus, mullite grains grow in the [001] direction for thermodynamic reasons[5].

Ceramic whiskers are commonly used as reinforcements in metal matrix composites (MMCS) and ceramic matrix composites (CMCS). For toughening of MMCS, it is required that high stresses are needed to fracture fibers at the tip of composite cracks and that the stress concentrations at the crack tips are as low as possible. In the whisker reinforced composites, high whisker stiffness implies high modulus at low temperature, which means both high modulus and high creep resistance under time-dependent deformation conditions at high temperature[6]. Mullite whiskers have unique properties which result from their near-perfect structure, and it can be used to improve the mechanical strength, the creep resistance, chemical stability and thermal properties[7-8]. Numerous methods have been developed to produce mullite whiskers[9-12], and most of them are expensive. Wang et al. synthesized CeO_2-doped mullite whiskers using sol-gel process[13], and the mullitization activation energies calculated based on non-isothermal differential scanning calorimetry (DSC) are 473 and 722 kJ·mol^{-1} for the 2%(*n*/*n*) CeO_2-doped and undoped samples, respectively. Kong et al.[14-15] obtained the anisotropic microstructure of mullite ceramics by high-energy ball milling method. Wang et al.[16-17] prepared mulllite whiskers with diameters ranging from 30 to 150 nm and lengths of over several microns through molten salts reactions. Mullite whiskers were also obtained by means of the thermal decomposition

of natural colorless topaz doped with rare earth oxides[18]. Molten salt reaction has been employed to synthesis ceramic powders because it decreases reaction temperature and gives powders of homogeneous morphology[19-20]. Molten salts provide liquid environment in which the nucleation and growth of grains are dependent on the dissolution of chemical reagents in the molten flux. Yang et al. prepared highly ordered mullite nanowhiskers using B_2O_3-doped molten salt synthesis method, and the reaction mechanism is attributed to local concentration gradient[21]. Zhu et al. studied the mullite growth mechanism using aluminum sulfate and silica as raw materials in molten sodium sulfate by the differential scanning calorimetry[22]. Zhang et al. synthesized mullite whiskers with $Al_2(SO_4)_3$ and $Al(OH)_3$ as alumina precursors by molten salt synthesis, and experimental result indicate that amorphous Al_2O_3 is beneficial for the formation of mullite[23]. When amorphous Al_2O_3 is produced by the decomposition reaction of $Al_2(SO_4)_3$, the total reaction processes are comprehensive and complicate paths included solid-liquid-gas phase transformation, the thermal pyrolysis mechanism of aluminum sulfate have been researched somewhat, but the decomposition reaction hasn't been extensively investigated from the thermodynamic and kinetic view.

Herein, mullite whiskers were prepared using kieselguhr or silica fume as silica precursors in molten salt system, and α-Al_2O_3 was also obtained in Na_2SO_4 flux through decomposition reaction of aluminum sulfate without silica involved in comprehensive reactions. Silica fume emerges as a by-product from the melting ferrosilicon alloy, and this solid waste presents serious problems of storing and environmental pollution. Kieselguhr is a kind of siliceous sedimentary rock originated from ancient biological cells, which can be used as thermal insulation materials, filler sand catalyst carriers in industry field. Although chemical composition, morphology and structure have great differences, SiO_2 is the mainly ingredients for silica fume and kieselguhr. Influence on the resulting product can be shown through different silica sources selecting, interesting for this contrast, the same product (mullite whiskers) was fabricated in our experiments. Decomposition kinetics of aluminum sulfate was explored using dynamic thermal analysis at different heating rates (β) of 5, 10 and 15 K·min^{-1}, respectively. Moreover, amorphous Al_2O_3 can be transformed into mullite phase because mullite is more stable state for Al_2O_3-SiO_2 eutectic phase while silica precursors are used as raw materials.

1　Experimental

1.1　Preparation

Selected silica fume (Xi′an Linyuan silica fume Ltd.) and kieselguhr (Tianjin Bodi Chemical Co., Ltd.) were used as the silica precursors to fabricate mullite whiskers, and physical parameters of kieselguhr and silica fume are listed in Table 1. $Al_2(SO_4)_3$ and Na_2SO_4 were weighed accurately according to the molar ratio of SiO_2, $Al_2(SO_4)_3$ and Na_2SO_4 (n_{SiO_2}:$n_{Al_2O_3}$:$n_{Na_2SO_4}$=6:1:10). The mixture was grinded in a ceramic mortar for 20 minutes, and then heated to final temperature of 800 ℃ (or 900 ℃) for 2 h. The samples were washed with hot water to remove sodium sulfate (non reacting solvent). Then, white mullite powders were obtained after filtration, washed and dried.

Amorphous alumina, composition of mullite ($3Al_2O_3·2SiO_2$), came from the pyrolysis of $Al_2(SO_4)_3$ in this experiment. In order to investigate the influence of aluminum sulfate, the product of $Al_2(SO_4)_3$ decomposition was obtained in molten salt system, and the preparation process is described as follows: Firstly, $Al_2(SO_4)_3$ and Na_2SO_4 were weighed accurately according to molar ratio of $Al_2(SO_4)_3$ to Na_2SO_4 being 1:5, and

Table 1　Physical parameters of kieselguhr and silica fume

Compound	w_{SiO_2} / %	w_{Cl} / %	S_{BET} / (m^2·g^{-1})	Density / (g·cm^{-3})
Kieselguhr	91.18	0.01	55	0.45
Silica fume	95.23	0.018	26	0.35

the mixed powder ($Al_2(SO_4)_3$+Na_2SO_4) was grinded in a ceramic mortar for 20 min. Subsequently, the mixed powders was placed in the bottom of alumina crucible and slowly heated to 900 ℃ for 2 h and then cooled down to room temperature in a furnace. Finally, the product was obtained after boiling in distilled water, filtration and drying.

1.2 Characterization

Crystalline phase of the sample was examined by using X-ray diffractometer (XRD, D/MAX-RA), with monochromated Cu $K\alpha$ radiation (λ =0.154 18 nm) operating at 40 kV and 30 mA, scanning range (2θ) from 10° to 80°. Scanning electronic microscope (SEM, S-4800) coupled with energy dispersive spectrometer (EDS, INCA-350) was used to characterize and analyze the microstructure, which was operated at 20 kV and 20 mA. High-resolution TEM (HRTEM) and selected area electron diffraction (SAED) were conducted on the JEOL-2100F to characterize the microstructures of the whiskers. The sizes and distributions of particles were analyzed using Malvern laser particle size analyzer (Mastersizer 2000). The decomposition of $Al_2(SO_4)_3$ was performed in a simultaneous thermogravimetry and differential scanning calorimetry (TG-DSC) (STA 449F5, Netzsch, Germany). About 15 mg of sample was taken in a platinum crucible and heated from 300 to 1 273 K in nitrogen environment with a constant flow rate of 40 mL·min^{-1} (with 99.99% purity) at different heating rates (β) being 5, 10 and 15 K·min^{-1}.

2 Results and discussion

2.1 XRD analysis

Fig.1 shows XRD patterns of final products using silica fume (or kieselguhr) as raw materials for molten salt synthesis. Mullite phase has been formed in the samples heated at 800 and 900 ℃, since there exist several strong peaks at 2θ=16.52°, 26.32°, 31.08°, 33.36°, 35.36°, 40.92° and 49.52°, which are attributed to the (111), (210), (001), (220), (111), (121) and (311) planes of the orthorhombic type (mullite) phase, respectively[24]. A series of peaks are showed in Fig.1a at 28.03°, 38.08°, 39.63°, 40.72° and 46.91°, which can be ascribed to the ($\bar{2}11$), ($\bar{2}02$), ($0\bar{2}2$), (220) and (131) planes of Al_2SiO_5, respectively. In addition, some weak peaks in Fig.1(b) were also checked out, which result from the impurities of kieselguhr.

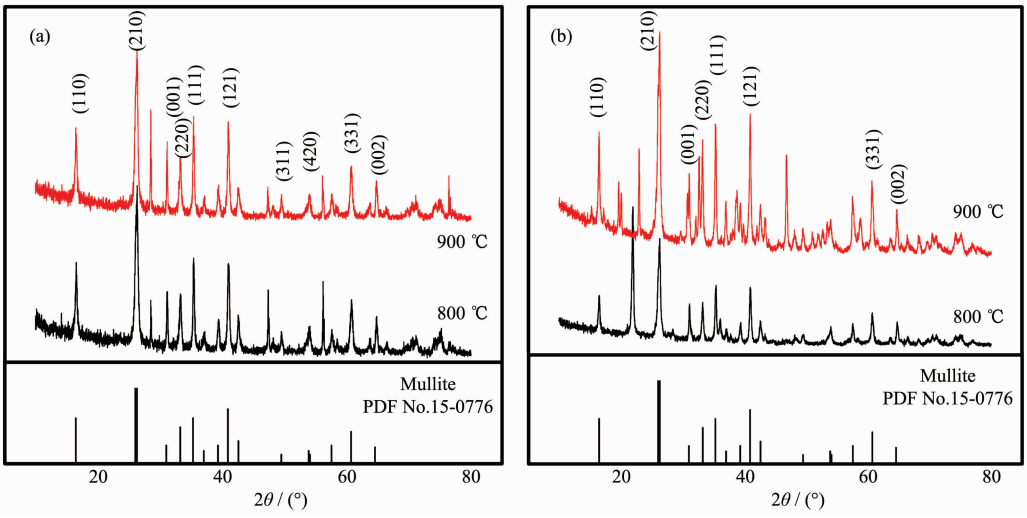

Fig.1 XRD patterns of mullite powders synthesized by silica fume (a) and kieselguhr (b)

2.2 SEM analysis

The SEM photographs and EDS spectra of prepared mullite whiskers are shown in Fig.2. It can be seen that the morphologies of samples (Fig.2a~b) synthesized at 800 ℃ are not perfect in comparison with the samples (Fig.2c, 2e) synthesized at 900 ℃. No matter which SiO_2-containing material is used, mullite whiskers will grow better at higher temperatures. Although the chemical composition of silica fume and kieselguhr is different, the final product is

mullite ($3Al_2O_3 \cdot 2SiO_2$) whiskers. It is well known that edge-shared AlO_6 octahedral chains align in the *c*-direction and are crosslinked by corner-shared (Si, Al)O_4 tetrahedra in unit cell of mullite crystal[25]. And the mullite crystal growth may be faster in crystallographic direction parallel to the c-axis than in other directions, resulting in a high degree of orientation. The whiskers that prepared at 800 and 900 ℃ both possess nanometer-sized diameters and micrometer-sized lengths. The corresponding EDS spectra of the whiskers fabricated from silica fume in Fig.2(d) and kieselguhr in Fig.2(f) indicate that the sample consist of Al, Si, O, Na, S and C. Moreover, the quantitative analysis shows that their average atomic ratio (n_{Al}:n_{Si}:n_O=6:2:13) approximates the stoichiometric ratio of mullite. The signals of elemental Na, S and C came from molten salts media (Na_2SO_4) and carbon-conductive tape for sample uploading.

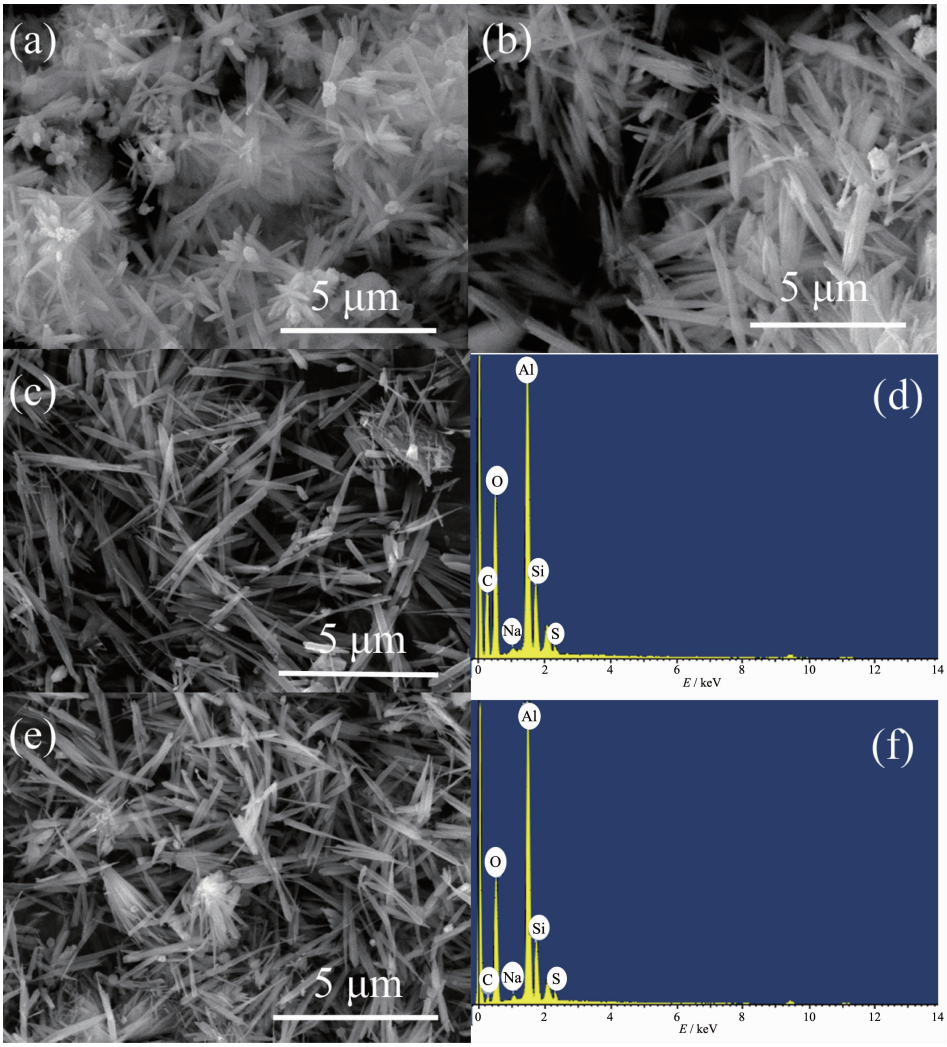

Fig.2　SEM micrographs and EDS spectra of the mullite whiskers prepared from silica fume at 800 ℃ (a), kieselguhr at 800 ℃ (b), silica fume at 900 ℃ (c~d) and kieselguhr at 900 ℃ (e~f)

2.3　TEM analysis

Fig.3 shows TEM image, HRTEM image and SAED pattern of the samples prepared from silica fume and kieselguhr. It can be seen that the average diameter of mullite whiskers was in a range of 50~150 nm and the length was over several microns. The selected-area electron diffraction patterns from the mullite whiskers in Fig.3(a,c) can be indexed to the orthorhombic structure. HRTEM image showed that the spacing was 0.539 nm, in accordance with (110) crystal plane spacing of mullite, which indicates that the mullite crystal grows along *c*-axis firstly and

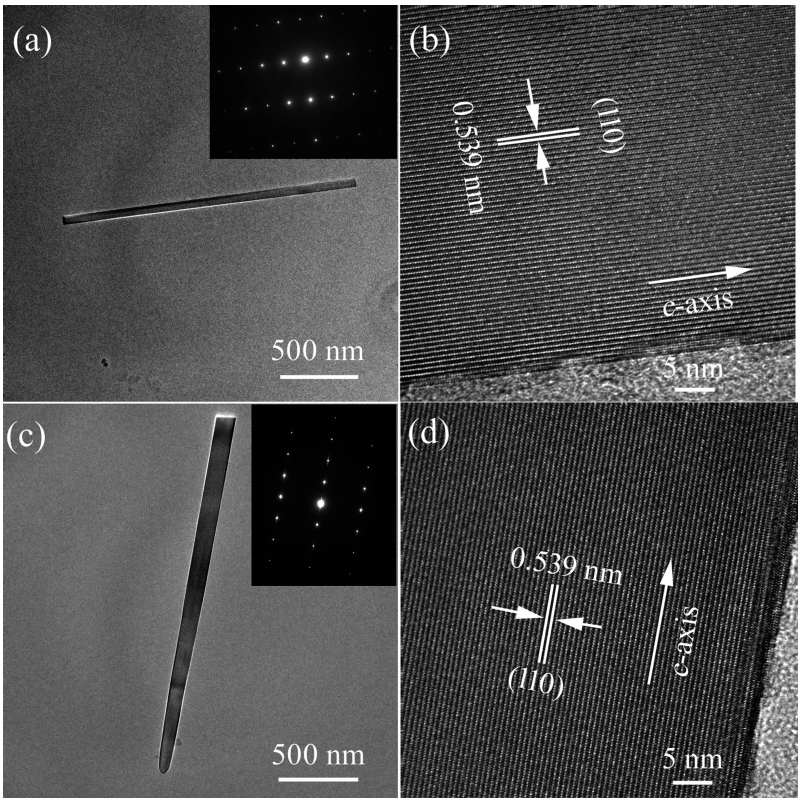

Inset: corresponding SAED pattern

Fig.3 TEM images(left) and HRTEM images(right) of mullite whiskers prepared from silica fume(a~b) and kieselguhr (c~d) at 900 ℃

develops into fibrous microstructure[26].

2.4 TG-DSC, XRD, SEM and particle size distributions analysis for aluminum sulfate decomposition

It can be seen that mullite whiskers formed in $Al_2(SO_4)_3$+Na_2SO_4 molten salts system using Kieselguhr or silica fume as silica precursors. If silica is not existed in molten sulfate flux, what will be happened in the system? According to some literatures[23], the decomposition reaction of $Al_2(SO_4)_3$ take place firstly and amorphous γ-Al_2O_3 forms above 700 ℃. In the second step, the γ-Al_2O_3 subsequently reacted with silica and transformed into other product. Therefore, two interesting questions are how the $Al_2(SO_4)_3$ is decomposed in sodium sulfate (non-reactive solvent) and how to analyze the resulting product to confirm this decomposition reaction mechanism.

Fig.4(a) shows the TG-DSC curve of aluminum sulfate octadecahydrate pyrolysis. It can be seen that the weight loss mainly takes place in the following three main ranges. The first weight loss (23.59%) is attributed to the dissociation of absorbed water from 75 to 150 ℃, and one endothermic peak appeared in the DSC curve simultaneously. The second one occured between 150 and 400 ℃ and the relevant weight loss ratio was 16.56%, which is ascribed to the removing of intramolecular crystal water. The third one (Weight loss: 37.60%) happened in a temperature range from 700 to 900 ℃, corresponding to an endothermic peak on the DSC curve, indicating that the decomposition of aluminum sulfate[23].

The synthesized product is characterized by X-ray diffraction (XRD) to determine phase. As can be seen from Fig.4(b), all of the diffraction peaks can be assigned to rhombohedral α-Al_2O_3 (PDF No.46-1212). No residue or contaminant has been detected, indicating the high purity of the sample[27]. Fig.4(c) presents the SEM image of α-Al_2O_3 particles, from which the α-Al_2O_3 is seen to be several hundred nanometers in diameter. Fig.4(d) shows the size distribution of as-synthesized α-Al_2O_3 particles. The average diameter was found to be 400~500 nm. Sodium sulfate is a

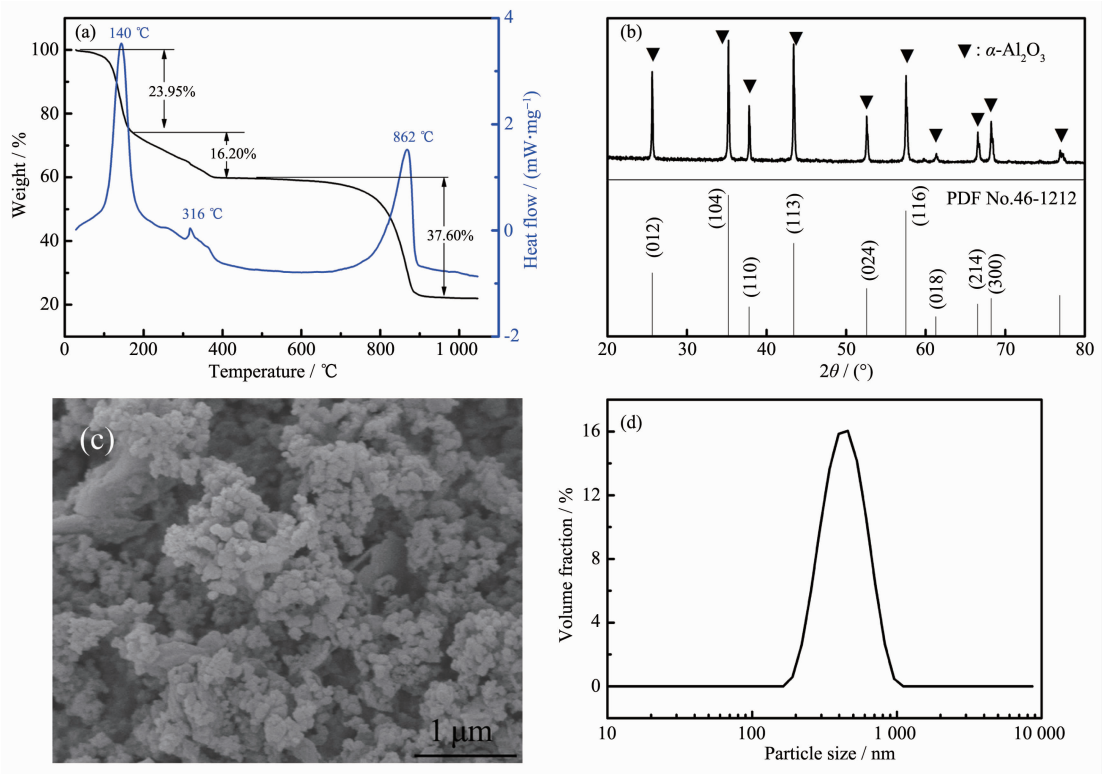

Fig.4　(a) TG-DSC curves of aluminum sulfate octadecahydrate decomposition; (b) XRD pattern of as-synthesized α-Al_2O_3 powders; (c) SEM morphology of as-synthesized α-Al_2O_3 powders; (d) Particle size distributions for α-Al_2O_3 powders

kind of high temperature solvent medium, which is beneficial for ion diffusion and stable phase growth. Amorphous alumina from $Al_2(SO_4)_3$ decomposition transformed into α-Al_2O_3 due to the lack of silica precursor.

2.5　TEM analysis of as-synthesized α-Al_2O_3 powder

Fig.5 shows TEM image, HRTEM image and SAED pattern of the as-synthesized α-Al_2O_3 powder. It can be seen that the width of this powder was in a range of 400~600 nm and the length was over one micron. The selected-area electron diffraction patterns in Fig.5(a) can be indexed to the rhombohedral crystal system. HRTEM image shows that the crystal plane spacing is 0.237 9 nm, in accordance with (110) crystal plane spacing of α-Al_2O_3, which confirms that α-Al_2O_3

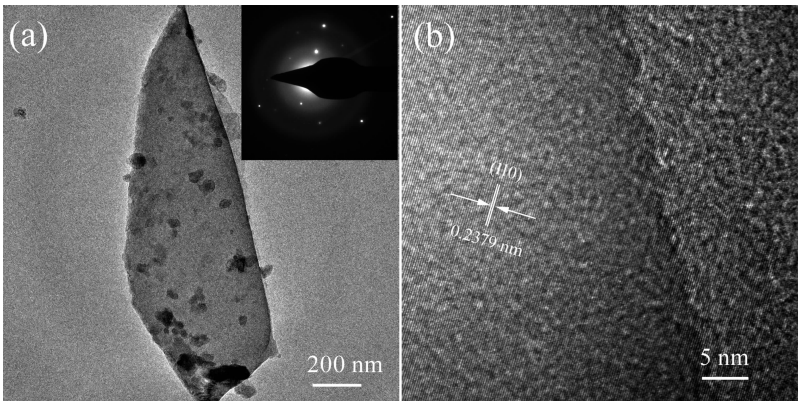

Inset: corresponding SAED pattern of the sample shown in (a)

Fig.5　(a) TEM image of individual α-Al_2O_3 powder after ultrasonic treatment; (b) HRTEM image of the powder

powder is formed in $Al_2(SO_4)_3$-Na_2SO_4 molten salt system.

2.6 Thermodynamic analysis

The utilization of aluminum sulfate thermal pyrolysis to prepare mullite whiskers has been researched somewhat[28], but the decomposition process hasn′t intensively been investigated from thermodynamic and kinetics point of view. Almost all the literatures think that amorphous γ-Al_2O_3 firstly forms in the liquid after decomposition of $Al_2(SO_4)_3$ according to reaction (**2**)[29-30]. But α-Al_2O_3 also forms as confirmed by the above mentioned characterization, indicating that α-Al_2O_3 phase derives from the decomposition reaction (**1**). According to traditional knowledge, the higher temperature is necessary for α-Al_2O_3 phase formation[31]. Thus, we try to explain α-Al_2O_3 formation through the thermal pyrolysis of $Al_2(SO_4)_3$ in high temperature solvent medium (Na_2SO_4) from the thermodynamic view.

$$Al_2(SO_4)_3\ (l) \rightarrow \alpha\text{-}Al_2O_3\ (s)+3SO_3\ (g) \quad (1)$$

$$Al_2(SO_4)_3\ (l) \rightarrow \gamma\text{-}Al_2O_3\ (s)+3SO_3\ (g) \quad (2)$$

The decomposition of $Al_2(SO_4)_3$ is controlled by pressure and temperature. For the reaction path (**1**) and (**2**), their free energy changes with temperature are shown in Fig.6, which is derived from $\Delta G=\Delta G^{\ominus}+\Delta nRT\ln(p/p^{\ominus})$ with $\Delta G^{\ominus}=\Delta H^{\ominus}-T\Delta S^{\ominus}$. As pressure and temperature are two interrelated variables about the reaction free energy change, the effect of pressure on the reaction free energy change is weak and the reaction free energy change (ΔG) can be calculated in $p=p^{\ominus}$ condition. Therefore, when $p=p^{\ominus}$ (constant pressure), $\Delta G=\Delta G^{\ominus}=\Delta H^{\ominus}-T\Delta S^{\ominus}$ with $\Delta H^{\ominus}=\Delta H_f^{\ominus}$($\alpha$-$Al_2O_3$ or γ-Al_2O_3)+$3\Delta H_f^{\ominus}(SO_3)-\Delta H_f^{\ominus}(Al_2(SO_4)_3)$ and $\Delta S^{\ominus}=S^{\ominus}$($\alpha$-$Al_2O_3$ or γ-Al_2O_3)+$3S^{\ominus}(SO_3)-S^{\ominus}(Al_2(SO_4)_3)$. The data of $\Delta H_f^{\ominus}$ and $S^{\ominus}$ are obtained from the reference[32]. The free energy changes (ΔG) of reaction (**1**) and reaction (**2**) with temperature are shown in Fig.6. The reaction path (**1**) could not happen in the lower temperature range ($\Delta G>0$), and the reaction would process vigorously when the temperature is up to 993 K ($\Delta G<0$). With the similar changing tendency, the equilibrium point of reaction path (**2**) is 1 023 K, and this chemical equilibrium could exist according to positive direction at higher temperature range (>1 023 K). It is well known that alumina exists in various stable and metastable phases[33], such as alumina hydrate ($Al_2O_3\cdot nH_2O$), transition state alumina (β-Al_2O_3, θ-Al_2O_3, η-Al_2O_3, γ-Al_2O_3, *etc*.) and stable phase alumina (α-Al_2O_3). Among them, the first two types are metastable phases. The metastable phases (β-Al_2O_3, θ-Al_2O_3, η-Al_2O_3, γ-Al_2O_3, *etc*.) can be converted into α-Al_2O_3 by high temperature sintering irreversibly.

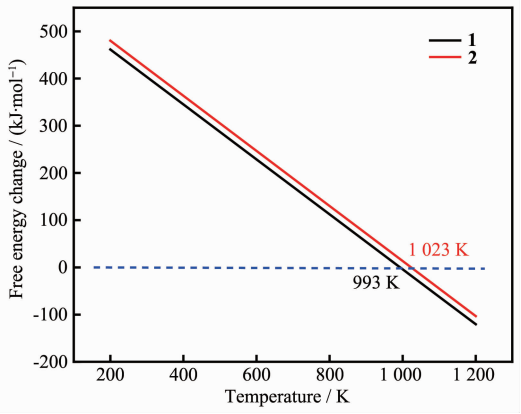

Fig.6 Changes of free energy ΔG for reactions (**1**) and (**2**) depending on temperature

It can been seen that γ-Al_2O_3 is a kind of metastable phase for alumina, in addition, γ-Al_2O_3 could be transformed into more stable mullite phase when some silica sources coexist in molten salt system. The reaction of mullite formation can be described as reaction (**3**).

$$3\gamma\text{-}Al_2O_3+2SiO_2 \rightarrow 3Al_2O_3\cdot 2SiO_2\ (\text{mullite}) \quad (3)$$

Where γ-Al_2O_3 comes from the decomposition of $Al_2(SO_4)_3$, and γ-Al_2O_3 subsequently transforms into mullite through Eq.(**3**), which is a commonly accepted mechanism of mullite formation. The mixture of γ-Al_2O_3 and SiO_2 is converted in a liquid molten salts environment, especially when they are intrinsic mixed in a molecular level. The reaction kinetic need not be considered because the diffusion paths of ingredient is so fast through the L-S growth mechanism[34]. Free energy change of reaction (**3**) reveal that mullite formation is a spontaneous process (Fig.7). Therefore, reaction (**1**), (**2**) and (**3**) should be considered together, and the decomposition of aluminum sulfate is the most

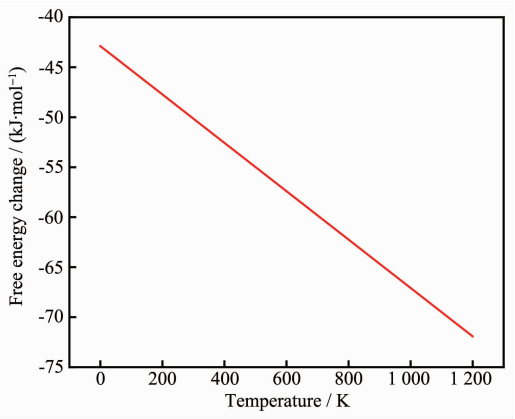

Fig.7　Change of free energy ΔG for reactions (**3**) depending on temperature

important controlling step.

In the $Al_2(SO_4)_3$-Na_2SO_4 molten salts, aluminum sulfate decomposition and transformation into γ-Al_2O_3 determine the growth rate of mullite whiskers. The γ-Al_2O_3 is more active in the molten salts system because the combination reaction (**3**) involves mullite formation. At the same time, mullite whiskers formation reaction can consume γ-Al_2O_3 and SiO_2, which accelerate the progress of reaction (**2**). The mullite whiskers growth mechanism can be described as follows: aluminum cations firstly exsit when temperature increase to the eutectic point ($Al_2(SO_4)_3$-Na_2SO_4), and then amorphous γ-Al_2O_3 is produced by the decomposition reaction of $Al_2(SO_4)_3$. Subsequently, SiO_2 coming from silica fume or kieselguhr can be dissolved in sulfate flux and the mullite nuclei are formed in this process. Then, mullite crystal grow quickly along the specific prismatic planes because it is the lowest surface energy barrier. The silica is consumed continuously in accordance with the above-mentioned combination reaction (**3**).

It is well known that the diffusion of Si^{4+} controlls densification and grain growth process of mullite whiskers[4]. Some literatures reveal that the needle-like shape is common to mullite formed in the presence of a liquid environment, and molten salts system provide a high ionic conductivity environment for crystal growth. Mullite whiskers growth requires the supply of silica species. In the absence of silica taking part in reactions, α-Al_2O_3 forms as the product of the decomposition of $Al_2(SO_4)_3$, while silica fume (or kieselguhr) is used as the starting reactant, then reaction (**3**) takes place in molten salts system, which eventually affects the decomposition of aluminum sulfate and the growth of mullite whiskers.

2.7　Kinetic analysis

In non-isothermal decomposition study, kinetic parameters are easily calculated from thermo-kinetic analysis. Among the integral methods, Kissinger-Akahira-Suno method gives more accurate apparent activation energy (E_a) as compared to other methods[35-36]. Therefore, different heating rates (β) of 5, 10 and 15 $K \cdot min^{-1}$ were selected to measure in this experiment and the apparent activation energy of $Al_2(SO_4)_3$ decomposition reaction was calculated using Kissinger-Akahira-Suno method. The equation is expressed as follows:

$$\ln(\beta/T_p^2)=\frac{E_a}{RT_p}+C \qquad (4)$$

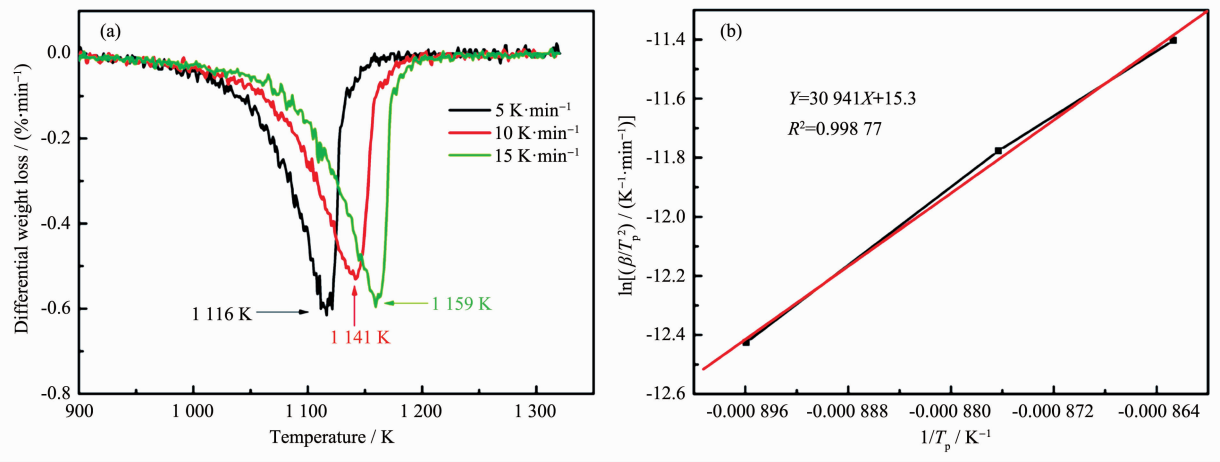

Fig.8　Plot of DTG vs T (a), ln (β/T_p^2) vs $1/T_p$ (b) for $Al_2(SO_4)_3$ decomposition reaction

Where E_a is the apparent activation energy and R is the gas constant, T denotes temperature, T_p is the peak temperature of DTG curves (Fig.8a) and β is the heating rate (β=dT/dt). Peak temperatures (T_p) appeared at 1 116, 1 141 and 1 159 K, which were ascribed to β=5, 10 and 15 K·min^{-1}, respectively. With the different heating rates, the plots (Fig.8b) of $\ln(\beta/T_p^2)$ against $1/T_p$ gave a straight line, and the slope of the corresponding line gave the value of apparent activation energy (Table 2). The apparent activation energy of $Al_2(SO_4)_3$ decomposition reaction is 257.2 kJ·mol^{-1}.

Table 2 Decomposition peak temperature and apparent activation energy for main decomposition of $Al_2(SO_4)_3$

β / (K·min^{-1})	T_p / K	E_a/R / K	E_a / (kJ·mol^{-1})
15	1 159		
10	1 141	3 094	257.2
5	1 116		

3 Conclusions

Mullite whiskers had been prepared by molten salt synthesis, and α-Al_2O_3 was formed in sulfate flux without silica species taking part in molten salt reactions. Aluminum sulfate decomposition and mullite formation reaction paths had been studied with thermodynamic and kinetic view. The main conclusions are summarized as follows:

(1) Mullite whiskers are single crystalline and possess uniform morphology with 200~400 nm in diameter and several microns in length. HRTEM image reveals that the interplanar spacing of 0.539 nm is in accordance with the spacing of the (110) crystal plane of mullite.

(2) According to the thermodynamic calculation, aluminum sulfate decomposition reaction is the most important controlling step, and α-Al_2O_3 form in sulfate flux at 720 ℃ without silica species introducing in raw materials.

(3) The apparent activation energy (E_a) of $Al_2(SO_4)_3$ decomposition is 257.2 kJ·mol^{-1} which is calculated through Kissinger-Akahira-Suno method with various heating rates (β=5, 10 and 15 K·min^{-1}).

References:

[1] Dong Y C, Feng X Y, Feng X F, et al. *J. Alloys Compd.*, **2008**,**460**(1/2):92-96

[2] Michel D, Colomban Ph, Abolhassani S, et al. *J. Eur. Ceram. Soc.*, **1996**,**16**(2):161-168

[3] Butler B D, Welberry T R. *J. Appl. Cryst.*, **1994**,**27**(5):742-754

[4] Ghate B B, Hasselmann D P H, Spriggs R M. *Ceram. Int.*, **1975**,**1**(3):105-110

[5] Zhang J H, Wu H D, Zhang S X, et al. *J. Cryst. Growth*, **2013**,**364**:11-15

[6] Wu M X, Messing G L. *J. Am. Ceram. Soc.*, **1994**,**77**(10):2586-2592

[7] Zhang H H, Zhang Y M, Wang B, et al. *Chem. Eng. J.*, **2015**,**268**:109-115

[8] Park Y M, Yang T Y, Yoon S Y, et al. *Mater. Sci. Eng. A*, **2007**,**454-455**:518-522

[9] Peng P, Sorrell C. *Mater. Lett.*, **2004**,**58**(7/8):1288-1291

[10]Ismail M G M U, Arai H, Nakai Z, et al. *J. Am. Ceram. Soc.*, **1990**,**73**(9):2736-2739

[11]Xu L F, Xi X A, Shui A Z, et al. *Ceram. Int.*, **2015**,**41**(9):11576-11579

[12]ZHANG Bing(张冰), CAO Chuan-Bao(曹传宝), XU Ya-Jie(许亚杰), et al. *Chinese J. Inorg. Chem.*(无机化学学报), **2005**,**21**(2):277-280

[13]Wang X, Li J H, Tong L X, et al. *Ceram. Int.*, **2013**,**39**(8):9677-9681

[14]Kong L B, Zhang T S, Ma J, et al. *Solid Sate Sci.*, **2009**,**11**(8):1333-1342

[15]Zhang T S, Kong L B, Du Z H, et al. *Scr. Mater.*, **2010**,**63**(11):1132-1135

[16]Wang W, Li H. W, Lai K R, et al. *J. Alloys Compd.*, **2012**,**510**(1):92-96

[17]Wang W, Hou G Y, Wang B Y, et al. *Mater. Chem. Phys.*, **2014**,**147**(1/2):198-203

[18]Monteiro R R, Sabioni A C S. *Ceram. Int.*, **2016**,**42**(1):49-55

[19]Wang G R, Liu Y, Ye J W, et al. *Mater. Lett.*, **2017**,**186**:361-363

[20]Elssfah E M, Song H S, Tang C C, et al. *Mater. Chem. Phys.*, **2007**,**101**(2/3):499-504

[21]Yang T, Chen J H, Li L D, et al. *Ceram. Int.*, **2015**,**41**(8):9560-9566

[22]ZHU Bo-Quan(朱伯铨), LI Xue-Dong(李雪冬), HAO Rui(郝瑞), et al. *Journal of Chinese Ceramic Society*(硅酸盐学报), **2006**,**34**:76-80

[23]Zhang P Y, Liu J C, Du H Y, et al. *J. Alloys Compd.*, **2010**,

491(1/2):447-451

[24]Sánchez-Soto P J, Eliche-Quesada D, Martínez-Martínez S, et al. *Mater. Lett.*, **2018**,**223**:154-158

[25]Jaaski J Y, Nissen H U. *Phys. Chem. Miner.*, **1983**,**10**(2):47-54

[26]JIANG Wei-Hui(江伟辉), PENG Yong-Feng(彭永烽), LIU Jian-Min(刘健敏), et al. *Journal of Inorganic Materials*(无机材料学报), **2010**,**25**(5):532-536

[27]Luan X Z, Li J H, Wang X. *Adv. Appl. Ceram.*, **2018**,**117**(4):248-254

[28]Zhang P Y, Liu J C, Du H Y, et al. *J. Alloys Compd.*, **2009**, **484**(1/2):580-584

[29]Kim B M, Cho Y K, Yoon S Y, et al. *Ceram. Int.*, **2005**,**35**(2):579-583

[30]Pelovski Y, Petkova V. *J. Therm. Anal.*, **1995**,**43**(1):339-349

[31]Kamruddin M, Ajikumar P K, Dash S, et al. *Thermochim. Acta*, **1996**,**287**(1):13-23

[32]Barin I. *Thermochemical Data of Pure Substances. Vol.*1, 2. 3*Ed*. Weinheim: Wiley-VCH, **1989**.

[33]Mo S D, Ching W Y. *Phys. Rev. B*: *Condens. Matter*, **1998**, **57**(15):219-228

[34]Saadi L, Moussa R, Samdi A, et al. *J. Eur. Ceram. Soc.*, **1999**,**19**(4):517-520

[35]HE Shui-Yang(何水样), YANG Rui(杨锐), CAO Wen-Kai(曹文凯), et al. *Acta Chim. Sinica*(化学学报), **2003**,**61**(5):715-720

[36]Kumar D, Maiti S C, Ghoroi C. *Thermochim. Acta*, **2016**, **624**:35-46